Quantum electronic transport through three-dimensional microconstrictions with variable shapes

A. G. Scherbakov, E. N. Bogachek, and Uzi Landman

School of Physics, Georgia Institute of Technology, Atlanta, Georgia 30332

(Received 8 September 1995)

The transport properties of three-dimensional quantum microconstrictions in field-free conditions and under the influence of magnetic fields of arbitrary strengths and directions are studied via a generalized Büttiker model [Phys. Rev. B **41**, 7906 (1990)]. It is shown that conductance quantization is influenced by the geometry of the microconstriction (that is, its length and the shape of its transverse cross section). In a weak longitudinal magnetic field, when $r_c \gg d$, where r_c is the cyclotron radius and d the effective transverse size of the narrowing of the microconstriction, the conductance exhibits Aharonov-Bohm–type behavior. This behavior transforms in the strong-field limit, $r_c \ll d$, into Shubnikov–de Haas oscillations with a superimposed Aharonov-Bohm fine structure. The dependence of the Aharonov-Bohm–type features on the length of the microconstriction and on temperature are demonstrated. Transverse magnetic fields lead to depopulation of the magnetoelectric subbands, resulting in a steplike decrease of the conductance upon increasing the strength of the applied magnetic field.

I. INTRODUCTION

Microconstrictions (sometimes referred to as point contacts) connecting massive reservoirs are unique objects for generation and investigation of ballistic quasiparticle transport in solids. Studies of such systems have been inspired by the pioneering investigations by Sharvin[1] in the mid-1960s. In early studies, three-dimensional (3D) metallic point contacts were fabricated usually by pressing a needle on a crystal face and were of submicron dimensions; that is, sizes which are large compared with the electron wavelength. The character of electronic transport under such conditions is of semiclassical nature. The most interesting phenomena observed in classical point contacts were electronic focusing[1] and point-contact spectroscopy of electron-phonon interactions.[2,3] Quantum effects in large metallic point contacts emerge in the presence of magnetic fields because of magnetic quantization in the reservoirs.[4,5]

Progress in modern nanotechnologies, such as molecular-beam epitaxy, made it possible to fabricate ballistic point contacts with continuously variable sizes in a two-dimensional (2D) electron gas (e.g., GaAs-Al$_x$Ga$_{1-x}$As heterostructures). The width of the opening in such structures can be of the same order as the electron Fermi wavelengths λ_F ($\lambda_F \simeq 400$ Å). Consequently, such point contacts can reveal quantum properties even under field-free conditions. Indeed it was found that the conductance of such 2D constrictions is quantized in units of $2e^2/h$, when the constriction size is varied.[6,7]

The physical origin of such a behavior of the conductance lies in the discrete character of the change in the number of transport modes (channels) which are transmitted through the constriction[8] (for a review, see Ref. 9). In the absence of a magnetic field the number of transmitted modes is determined by the minimal width of the constriction. Because of the 2D character of the electronic transport, the influence of magnetic fields is significant only in the strong-field limit (the quantum-Hall-effect regime) where charge transport occurs via edge states. The edge states localized near the boundaries effectively form a doubly connected region in a simply connected constriction, resulting in the appearance of Aharonov-Bohm (AB) oscillations (hc/e oscillations) in the conductance,[10,11] in accordance with previous ideas pertaining to the manifestation of the AB effect in simply connected geometries.[12–14]

The phenomenon of conductance quantization is not restricted to 2D constrictions, and under appropriate conditions it should also occur in 3D metallic point contacts with small constriction diameters. Early molecular-dynamics simulations[15,16] have shown that such three-dimensional junctions form between two materials bodies brought into close proximity, and that subsequent retraction of the two contacting bodies results in elongation of the contact and generation of a stretched 3D constriction (connective wire). These simulations have revealed the plastic nature of the elongation process of such metallic wires (which in the case of gold were predicted to be characterized by a critical yield stress of ~ 2–3 Gpa, i.e., an order of magnitude larger than that of bulk Au), occurring in a sequence of stress-accumulation and stress-relief stages, and leading to the formation of highly ordered crystalline wires. Furthermore, it was shown that the extent of such pulled wires can be controlled (e.g., indentation of a tip into a substrate and subsequent retraction[15]), and that crystalline nanoscale wires (nanowires) are formed at the later stages of the elongation process, irrespective of the initial size of the contact. Additionally, it was suggested that these systems could be used for investigations of quantum effects in electronic transport through nanowires and single-atom point contacts.[15] Electronic conductance in such 3D constrictions has been theoretically analyzed[17–19] using various models (e.g., contacts with symmetric cross sections characterized by hard walls, i.e., an infinite confining potential, with adiabatically varying shape, and in the limit of weak magnetic fields).

The use of scanning tunneling microscopy (STM) for fabrication of atomic-size metallic contacts (nanowires) and measurement of their properties, opened new avenues for studies of 3D quantum constrictions. Indeed, measurements

of the electric properties of such constrictions, made with a gold tip and sample, revealed room-temperature conductance quantization in multiples of $2e^2/h$ when the contact was elongated.[20,21] Similar results have been reported using STM in ultrahigh vacuum at room temperature with nickel, copper, and platinum samples,[22] and at cyrogenic conditions with lead,[23] as well as in measurements employing a mechanically controllable break-junction technique.[24]

In this paper we present a theory of electronic transport through a 3D ballistic microconstriction in field-free conditions and under the influence of applied magnetic fields. To this end we model the system via a generalized Büttiker model, originally introduced for studies of transport in 2D systems.[25,26] This model, where the constriction is characterized by a soft-wall confining potential, allows us to investigate the role of the shape of the constriction, including anisotropy effects, and the influence of magnetic fields of arbitrary strengths and directions. We demonstrate that the properties of 3D quantum contacts may differ significantly from those found in 2D constrictions. The character of conductance quantization occurring in long 3D constrictions depends on the shape of the cross section of the contact. In symmetric contacts (i.e., circular cross section) the height of the steps, measured in units of $2e^2/h$, is proportional to the degree of degeneracy of the transverse energy levels. In asymmetric cases (i.e., ellipsoidal cross sections), with nondegenerate energy levels, or a reduced degree of degeneracy, the steplike structure may be obliterated (smeared).

Application of a magnetic field alters the character of electronic transport through the constriction, since the presence of an additional parameter of length dimension, i.e., the cyclotron radius r_c, leads to the emergence of different transport regimes. For a longitudinal orientation of the magnetic field with respect to the axis of the microconstriction, the conductance behavior is different in two field-strength regimes: (i) a weak-field regime, $r_c > d$, and (ii) a strong-field regime $r_c < d$, where d is the typical transverse size of the narrowing. In the first case the longitudinal motion of the electron occurs via edge states (surface states), resulting in the appearance of an AB-type structure in the conductance (compare with Refs. 12 and 13). In the other limit (strong field), electronic transport occurs both via edge states and "bulk (Landau)" states (see below). As a result the conductance exhibits strong Shubnikov–de Haas oscillations with a superimposed AB-type fine structure. Increase of the temperature leads to the disappearance of the AB conductance oscillations, first in the region of strong magnetic fields, and then, at higher temperatures, in the region of weak ones.

For a transverse orientation (perpendicular to the axis of the microconstriction) of the applied magnetic field only the edge states are current carrying. In this case, increase of the magnetic field leads to a decrease of the number of occupied magnetoelectric subbands corresponding to the edge modes (so-called magnetic depopulation of the subbands), resulting in a steplike decrease of the conductance.

The paper is organized as follows. In Sec. II, we discuss the model used to describe 3D constrictions of arbitrary shapes, and calculate the conductance both in the magnetic-field-free case and in magnetic fields with longitudinal, transverse, and tilted orientations. We summarize our results in Sec. III.
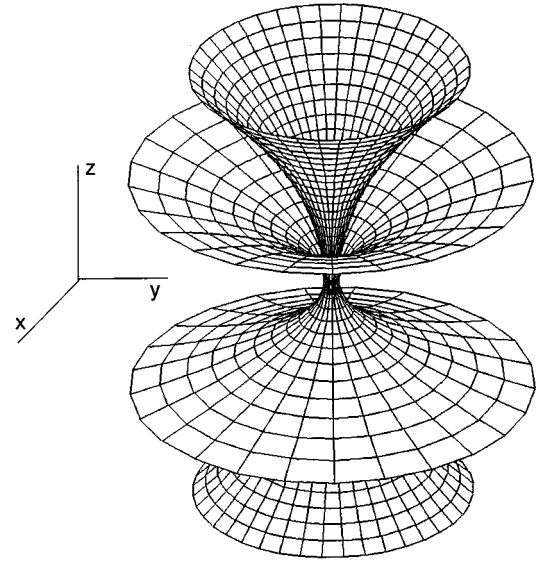

FIG. 1. Equipotential surfaces for the confining potential [see Eq. (1)] modeling a three-dimensional constriction (contact), drawn for the cases of a short symmetric ($\omega_x = \omega_y$) constriction, and a longer one (that is, same values for ω_x and ω_y, and a smaller value of ω_z).

II. MODEL AND RESULTS

We consider ballistic electronic transport through 3D constrictions modeled by a confining potential which characterizes the shape and extent of the constriction. In such systems the only source for resistance is of geometric (shape) origin. We model the confining potential by a smooth function. Near the bottleneck (the narrowest part) of the constriction, the confining model potential may be expanded, and to second order in the coordinates (x,y,z) it can be expressed in the following form:

$$V(x,y,z) = V_0 - \tfrac{1}{2}m^*\omega_z^2 z^2 + \tfrac{1}{2}m^*(\omega_x^2 x^2 + \omega_y^2 y^2). \quad (1)$$

Here z is the coordinate along the constriction axis, x and y are the coordinates in the transverse directions, V_0 is the potential at the saddle point, and m^* is the effective mass of the electron. The shape of the potential (defining the constriction) is determined by the terms containing the frequencies ω_x, ω_y, and ω_z; examples of equipotential surfaces for different values of the ratio of ω_x and ω_y to ω_z are shown in Fig. 1. Larger values of the ratio correspond to longer constrictions with smaller apertures. The parameters ω_x/ω_y describes the degree of anisotropy of the cross section of the constriction.

A. Magnetic-field-free case

We consider first the magnetic-field-free case, where the total Hamiltonian is given by

$$\mathcal{H} = -\frac{\hbar^2}{2m^*}\Delta + V(x,y,z). \quad (2)$$

Expressing the wave function ψ in the form

$$\psi(x,y,z) = R(x,y)Z(z), \quad (3)$$

and separating the transverse and longitudinal variables in the Schrödinger equation we obtain the equation describing the motion of the electron through the constriction (z direction)

$$-\frac{\hbar^2}{2m^*}\frac{\partial^2 z}{\partial z^2}+V_{n_1 n_2}^{\text{eff}}(z)Z=EZ, \qquad (4)$$

where

$$V_{n_1 n_2}^{\text{eff}}(z)=V_0+E_{n_1 n_2}-\tfrac{1}{2}m^*\omega_z^2 z^2 \qquad (5)$$

is the effective potential, and

$$E_{n_1 n_2}=\hbar\omega_x(n_1+\tfrac{1}{2})+\hbar\omega_y(n_2+\tfrac{1}{2}) \qquad (6)$$

are transverse electronic levels in the narrowest part of the constriction (at the plane $z=0$), E is the total energy, and n_1 and n_2 are non-negative integers. The effective potential $V_{n_1 n_2}^{\text{eff}}(z)$ may be considered as the band bottom of the n_1, n_2 quantum channel.[8,25] In the absence of tunneling the threshold energy for each channel at the plane $z=0$, is equal to $V_{n_1 n_2}^{\text{eff}}(0)$. Channels with energies $E>V_{n_1 n_2}^{\text{eff}}(0)$ pass through the constriction with unit probability, while those with $E<V_{n_1 n_2}^{\text{eff}}(0)$ are reflected. Consequently, in this case, the transmission probability (and thus the conductance) is a sharp-edge stepwise function of the total energy. Effects of electronic tunneling through the effective potential [Eq. (5)] lead to a "smearing" of the threshold energy, thus affecting the transmission probability in the vicinity of the rises of the conductance steps. In this case the transmission probability for the incident channel n_1, n_2 has the form[27]

$$T_{n_1 n_2;n_1' n_2'}=\delta_{n_1 n_1'}\delta_{n_2 n_2'}[1+\exp(-2\pi\epsilon_{n_1 n_2})]^{-1}, \qquad (7)$$

where

$$\epsilon_{n_1 n_2}=\frac{E-V_0-E_{n_1 n_2}}{\hbar\omega_z}. \qquad (8)$$

It is of importance to note that because of the harmonic form of the potential there is no mode mixing during the tunneling process. As in the case of 2D constrictions,[25,26] the effective length of the three-dimensional narrowing is determined by the frequency ω_z which influences the smearing of the conductance steps.

The conductance of the constriction is determined by a Landauer-type formula[28,29]

$$G=\frac{2e^2}{h}\sum_{n_1,n_2}T_{n_1 n_2,n_1 n_2}, \qquad (9)$$

where the sum runs over all transmitted channels.

Consider first a symmetric case $\omega_x=\omega_y=\omega_0$ (a constriction with a circular cross section). The conductance of such a system as a function of the normalized energy, $\xi=(E-V_0)/\hbar\omega_z$, for different values of the dimensionless parameter ω_0/ω_z is plotted in Fig. 2. At large values of ω_0/ω_z, corresponding to long constrictions with smaller apertures, the conductance has a well-defined steplike structure which is destroyed with decreasing values of ω_0/ω_z. Such a behavior is in correspondence with a similar dependence of
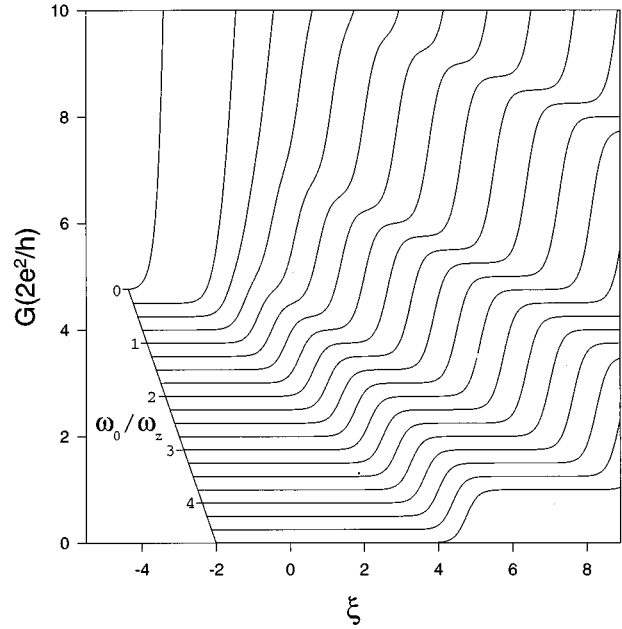

FIG. 2. Conductance G (in units of $2e^2/h$) of three-dimensional symmetric constrictions ($\omega_x=\omega_y=\omega_0$), vs $\xi=(E-V_0)/\hbar\omega_z$, plotted for various values of ω_0/ω_z. Note that the quantization of the conductance disappears for short constrictions, i.e., $\omega_0/\omega_z\lesssim 1$. Note also that the height of the steps varies with the step number, i.e., the height $2e^2/h$ for the first step, $2(2e^2/h)$ for the second one, and so on.

the conductance of 2D and 3D quantum contacts which were studied using different models.[17,18,25,26]

Degeneracies of the transverse energy levels in symmetric contacts lead to an increase of the step height (Fig. 2). The heights of the steps (i.e., rises), in fundamental units of $2e^2/h$, are proportional to the degree of degeneracy, n, which in our model is determined by the sum of quantum numbers, $n=n_1+n_2+1$.

The slopes of the rises of the steps and of their plateaus are determined by the expression

$$\frac{dG}{dE}=\frac{2e^2}{h}\frac{\pi}{2\hbar\omega_z}\sum_{n_1,n_2}[\cosh^2(\pi\epsilon_{n_1 n_2})]^{-1}, \qquad (10)$$

which is plotted in the inset to Fig. 3. This quantity can be used to characterize the "quality" of the conductance quantization.[25]

The conductance steps exhibit maximum values of the slopes at the centers of the step rises, corresponding to the classical (i.e., in the absence of tunneling) threshold energies $E=E_{n_1 n_2}+V_0$ [Eqs. (5) and (6)]. The magnitude of the maximum slope of the rise of the nth step is

$$\left(\frac{dG}{dE}\right)_{\text{max}}\simeq n\frac{2e^2}{h}\frac{\pi}{2\hbar\omega_z}, \qquad (11)$$

which increases with the degree of degeneracy n (see the inset to Fig. 3). The slopes of the rises of the steps and those of the plateaus also depend on the frequency ω_z [see Eq. (10)]. For $\omega_0\gg\omega_z$ the slope of the plateau between the nth and $(n+1)$th steps, with $n=n_1+n_2+1$ and $n+1$ degrees of degeneracy, respectively, is minimal at the energy
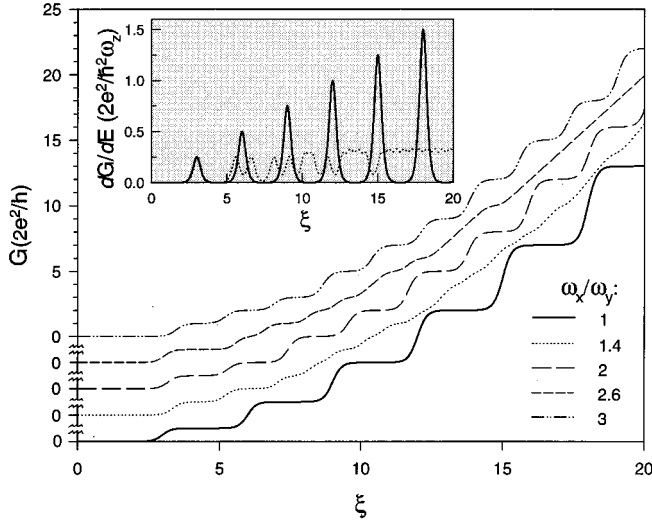
FIG. 3. Conductance (G, in units of $2e^2/h$) vs ξ for symmetric ($\omega_x = \omega_y$) and asymmetric ($\omega_x \neq \omega_y$) constrictions, with a constant cross-sectional area, i.e., $\omega_x \omega_y = \text{const}$. The plots shown in this figure as well as in Figs. 4, 5, 8, 9, and 10, were calculated for $\omega_0/\omega_z = 3$, where $\omega_0 = \sqrt{\omega_x \omega_y}$, corresponding to the symmetric case with $\omega_0/\omega_z = 3$ in Fig. 2. For values of ω_x and ω_y such that ω_x/ω_y is irrational or can be expressed as the ratio of two large integers, the quantization of G is obliterated; e.g., see curves for $\omega_x/\omega_y = 1.4$ and 2.6. In the inset the derivative of G, $\partial G/\partial E$, is plotted vs ξ for the cases of $\omega_x/\omega_y = 1$ (solid line) and $\omega_x/\omega_y = 1.4$ (dotted line).

$$E(X) \simeq V_0 + \hbar \omega_0 (n_1 + n_2 + 1 + X), \qquad (12a)$$

$$X = \frac{1}{2} - \frac{1}{4\pi} \frac{\omega_z}{\omega_0} \ln\left(\frac{n+1}{n}\right). \qquad (12b)$$

The minimal slope of the plateau, obtained by evaluating Eq. (10) using Eq. (12), is given by

$$\left(\frac{dG}{dE}\right)_{\min} \simeq \frac{2e^2}{h} \frac{2\pi}{\hbar \omega_z} [n \, \exp(-2\pi\omega_0 X/\omega_z)$$
$$+ (n+1)\exp(-2\pi\omega_0(1-X)/\omega_z)]. \quad (13)$$

In asymmetric constrictions ($\omega_x \neq \omega_y$) the degeneracy of the transverse levels is lifted, and consequently increases in the heights of the steps (i.e., larger step rises) may occur, for the harmonic model confining potential used by us here, under the following condition:

$$\gamma_x \omega_x + \gamma_y \omega_y = 0, \qquad (14)$$

where γ_x and γ_y are integers. As aforementioned, the shape of the cross section of the constriction is determined by the parameter ω_x/ω_y, with $\omega_x/\omega_y = 1$ corresponding to a circular shape. For a decrease in the degree of degeneracy n, or in the absence of degeneracy (i.e., $n=1$), the lengths of the plateaus (i.e., the width of the flat portions of the conductance) between successive steps decrease, because a step corresponding to a degenerate energy level (channel) is split into several steps due to lifting of the degeneracy. At the same time the slopes of the step rises also decrease because of the degeneracy index n in Eq. (11) (note that the frequency ω_z is constant). When the "smearing region" of the

steps becomes comparable to the size of the intervening plateaus, the steplike character may disappear; see the curve in Fig. 3 which depicts the conductance and its derivative (i.e., the slope, shown in the inset), as functions of the normalized energy ξ for different values of ω_x/ω_y, while maintaining a constant value of the cross-sectional area of the constriction, i.e., $\omega_x \omega_y$ is held constant (with this condition, for a given ξ the classical conductance value in zero field[1] is the same for all values of ω_x/ω_y since it depends on the cross-sectional area of the constriction and not on its shape). Obviously, the effect of the cross-sectional asymmetry on the quality of the conductance quantization steps is larger for shorter constrictions (characterized in our model by smaller values of ω_0/ω_z; see Fig. 2), and its influence increases for larger energies. It is interesting to remark in this context that, as mentioned above, it has been shown by molecular-dynamics simulations[15,16] that the process of formation and elongation of a three-dimensional constriction involves ordered and disordered stages occurring in the "necking" region of the pulled wires. Moreover, variations in the shapes of the cross section of such 3D wires in various ordered states have been observed. Such variations may explain the disappearance of some of the conductance steps during the elongation process which were observed in experimental measurements performed on 3D quantum contacts (gold nanowires).[21]

B. Longitudinal, transverse, and tilted magnetic fields

In this subsection, we analyze electronic transport through the constriction in the presence of a magnetic field. In this case the total Hamiltonian is given by

$$\mathscr{H} = \frac{1}{2m^*} \left(\vec{p} - \frac{e}{c}\vec{A}\right)^2 + V(x,y,z). \qquad (15)$$

1. Longitudinal magnetic fields

First we consider the case of longitudinal orientation of the magnetic field ($H \| z$) with the symmetric gauge for the vector potential

$$\vec{A} = \tfrac{1}{2}(-Hy, Hx, 0). \qquad (16)$$

As in the previous case of zero magnetic field, we can separate the variables for longitudinal and transverse motion. In a magnetic field we obtain for the transverse energy levels the expression[30]

$$E^H_{n_1 n_2} = \hbar \omega_+ (n_1 + \tfrac{1}{2}) + \hbar \omega_- (n_2 + \tfrac{1}{2}) \qquad (17)$$

and

$$\omega_\pm = \tfrac{1}{2}\left[\sqrt{\Omega^2 + (\omega_x + \omega_y)^2} \pm \sqrt{\Omega^2 + (\omega_x - \omega_y)^2}\right], \quad (18)$$

where n_1 and n_2 are non-negative integers, and $\Omega = eH/m^*c$ is the cyclotron frequency. A longitudinal magnetic field renormalizes the effective transverse frequencies $\omega_\pm$, and does not affect the longitudinal frequency ω_z. The energy levels $E^H_{n_1 n_2}$ given by Eqs. (17) and (18) transform to Eq. (6) for $H=0$, and to the Fock-Darwin levels[31] in the symmetric case $\omega_x = \omega_y = \omega_0$. The conductance of a 3D con-

striction in a longitudinal magnetic field is determined by Eqs. (7), (8), and (9) with $E^H_{n_1 n_2}$ replacing $E_{n_1 n_2}$.

The confining potential in the plane perpendicular to the axis of the contact removes the degeneracy of the bulk energy levels which depend on both quantum numbers n_1, n_2 and the potential parameters ω_x, ω_y describing the cross-sectional shape of the constriction. This means that all the energy levels correspond to surface states, for all values of the applied magnetic field, and form magnetoelectric subbands. Nevertheless, in strong magnetic fields, $\Omega \gg \omega_0$ (i.e., when the cyclotron radius $r_c = cm^* v_F / eH$ is much smaller than the effective transverse radius of the narrowing $d = v_F / \omega_0$, where v_F is the Fermi velocity) the spacings between electronic energy levels with different values of the quantum number n_1 is, to a first approximation with respect to the parameter ω_0 / Ω, proportional to the cyclotron frequency Ω, as for proper Landau levels.

Magnetic fields influence the conductance of the microconstriction in a significant manner. Because of the renormalization of the transverse frequencies in the presence of a magnetic field, an otherwise symmetric constriction becomes effectively asymmetric. In some sense the influence of the magnetic field is equivalent to the appearance of an anisotropy. In Fig. 4 we display the dependence of the conductance of a symmetric constriction $\omega_x = \omega_y = \omega_0$ on the normalized energy ξ for different values of the magnetic fields in the weak, $\Omega \ll \omega_0$ [see Fig. 4(a)], and strong, $\Omega \gg \omega_0$ [see Fig. 4(b)], limits. The removal of the degeneracy of the transverse electronic levels by the magnetic field decreases the slopes of the step rises, and may even lead to their disappearance.

It is of interest to investigate the magnetic-field dependence of the conductance for fixed parameters of the constriction. Such a dependence is shown in Fig. 5 for $\omega_0 / \omega_z = 3.0$ and different values of the parameter $\xi = (E - V_0) / \hbar \omega_z$. For weak fields, $\Omega < \omega_0$, well-pronounced oscillations of the AB type are observed. These oscillations are due to edge states described by Eqs. (17) and (18). Increasing the strength of the magnetic field causes a change in the number of allowed edge states in the narrowing, which is manifested by an oscillatory behavior of the conductance. In cylindrical channels with hard potential walls a similar mechanism leads, in a weak magnetic field, to the appearance of a sharp steplike structure of the conductance.[19] The inset in Fig. 5 portrays the Aharonov-Bohm oscillations for different but relatively close values of the parameter $\xi = (E - V_0) / \hbar \omega_z$. While in the presence of a magnetic field the conductance is of similar magnitude to that found for the magnetic-field-free case, its behavior is markedly modified. Different values of the parameter ξ correspond to slight changes of the constriction shape. For each shape of the constriction these oscillations are reproducible and form "magnetic fingerprints" of the constriction (see the inset to Fig. 5).

For stronger magnetic fields $\Omega > \omega_0$ (in this region the cyclotron radius becomes smaller than the effective size of the narrowing) the formation of "quasi-Landau orbits" in the constriction leads to the appearance of Shubnikov–de Haas oscillations. In this range of magnetic fields the aforementioned AB oscillations occur with significantly smaller amplitudes and periods, and they are superimposed on the
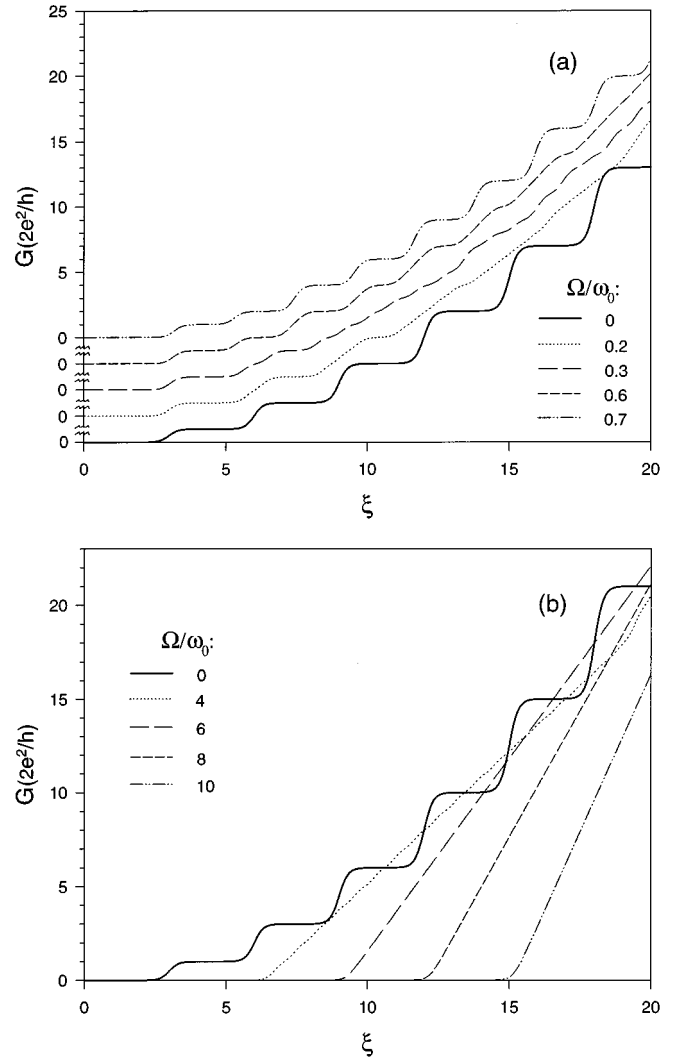

FIG. 4. Conductance (G, in units of $2e^2/h$) vs ξ, for symmetric constrictions ($\omega_x = \omega_y = \omega_0$) in the presence of applied longitudinal magnetic fields. In (a) the regime of weak magnetic fields is shown, i.e., $\Omega / \omega_0 < 1$, where Ω is the cyclotron frequency. Note the similarity of the behavior of the conductance to that shown for asymmetric constrictions in the field free case in Fig. 3, i.e., the disappearance of the conductance quantization for certain values of Ω / ω_0. In (b) we show the behavior of G in the regime of large longitudinal magnetic fields (the case of a vanishing field, $\Omega / \omega_0 = 0$, is included for comparison). The disappearance of the quantization of the conductance is evident. Note that change in the slope of G for large value of ξ, seen for the case of $\Omega / \omega_0 = 4$ [similarly, such changes of slope occur at even higher values of ξ for the curves corresponding to stronger applied fields. The origin of such changes in slope can be found from examination of the energy spectrum given in Eqs. (17) and (18)]. Similar changes in slope with increasing values of ξ can also be obtained for asymmetric constrictions under field-free conditions (Fig. 3) for high degrees of the asymmetry.

Shubnikov–de Haas ones. Moreover, the amplitude of the AB-type features in the conductance decreases with the increase of the magnetic field, unlike that of the Shubnikov–de Haas effect. (The possible coexistence of de Haas–van Alphen and AB oscillations in 2D systems with a dot or antidot has been discussed in Refs. 32–34.)
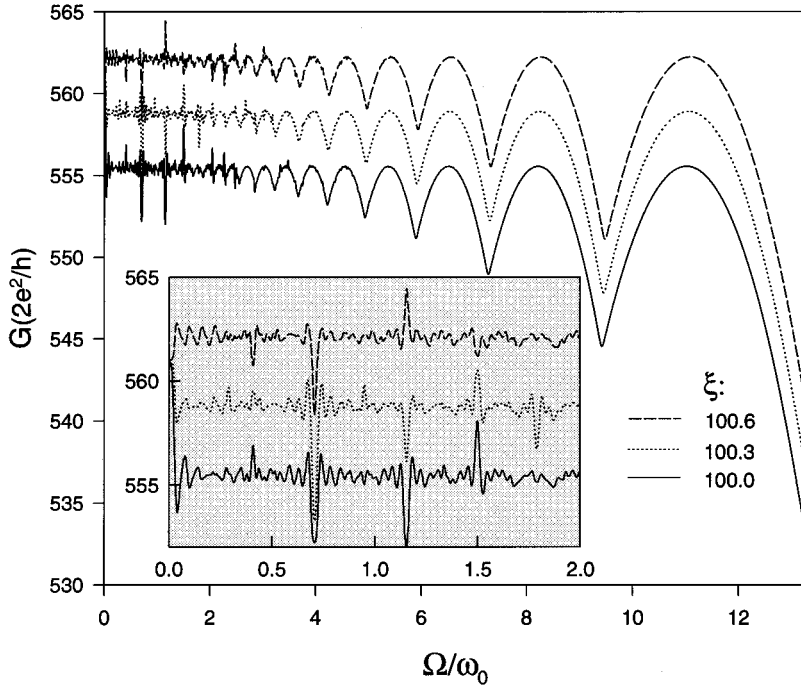
FIG. 5. Conductance (G, in units of $2e^2/h$) of 3D symmetric constrictions vs cyclotron frequency (Ω, in units of ω_0) for a longitudinal applied magnetic field. The curves correspond to different close values of the parameter ξ. The AB-type oscillations occurring at low fields, $\Omega \lesssim \omega_0$, transform for high fields into the Shubnikov−de Haas oscillations with a superimposed AB fine structure. Different values of ξ, corresponding to slight changes of the shape of the constriction, result in significant changes in the appearance of the AB oscillations (see the inset, where a magnified view of the region $0 \leq \Omega/\omega_0 \leq 2$ is shown).

The character of the magnetic oscillations of the conductance depends on the effective length of the microconstriction which is determined by the ratio ω_0/ω_z. The conductance plotted in Fig. 5 corresponds to a long contact $\omega_0/\omega_z = 3.0$ with a well-defined quantized structure (see Fig. 2). The two types of magnetic oscillations discussed above (the AB type and the Shubnikov−de Haas one) are due to edge states in the constriction and bulk states, respectively. Short enough constrictions, $\omega_0/\omega_z \ll 1$, cannot support stable edge states in a longitudinal field, and consequently the AB fine structure in the conductance dependence on the magnetic field disappears (Fig. 6). However, the Shubnikov−de Haas oscillations remain without change.[4] Note that in 3D constrictions placed in a longitudinal magnetic field, conductance quantization and AB oscillations may coexist, unlike the case of 2D contacts where backscattering processes, re-

quired for the occurrence of the AB oscillations, destroy the quantization (see, e.g., Ref. 26). Elongation of the constriction leads to increase of the AB contribution (Fig. 6). The appearance of beats in the AB structure is due to the interference of different edge channels contributing to the AB effect. A related mechanism leading to beats in the thermodynamic and transport characteristics of a 2D electron-gas system with an antidot was discussed in Refs. 34 and 35.

In the above we discussed the conductance behavior at zero temperature. To consider thermal effects we should substitute Eq. (9) for the conductance by the following equation:

$$G = \frac{2e^2}{h} \int d\epsilon \left(-\frac{\partial f_0}{\partial \epsilon} \right) \sum_{n_1, n_2} T_{n_1 n_2, n_1 n_2}, \qquad (19)$$
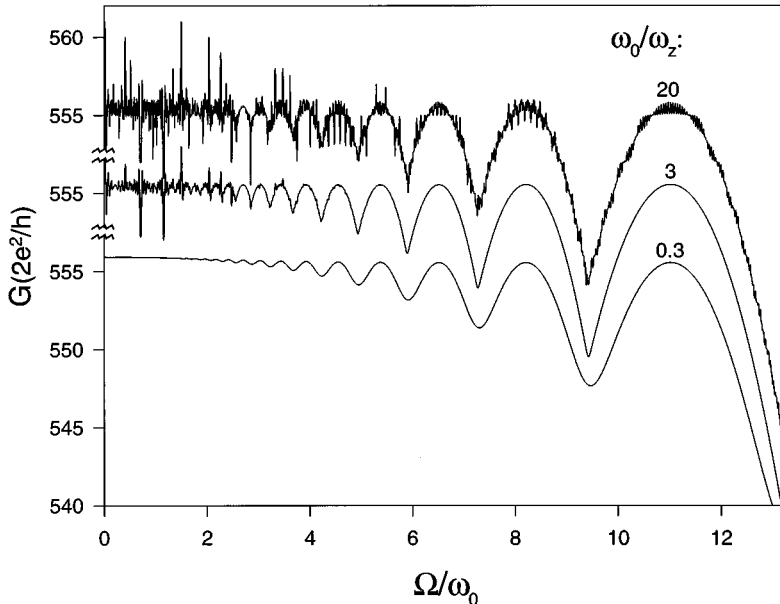

FIG. 6. Conductance (G, in units of $2e^2/h$) of 3D symmetric contacts vs cyclotron frequency (Ω, in units of ω_0), plotted for various values of the parameter ω_0/ω_z which controls the relative length of the constriction, and for a fixed value of the electron energy E, such that $(\omega_0/\omega_z)/\xi = 0.03$. Note the disappearance of the AB oscillations in short constrictions (small values of ω_0/ω_z).
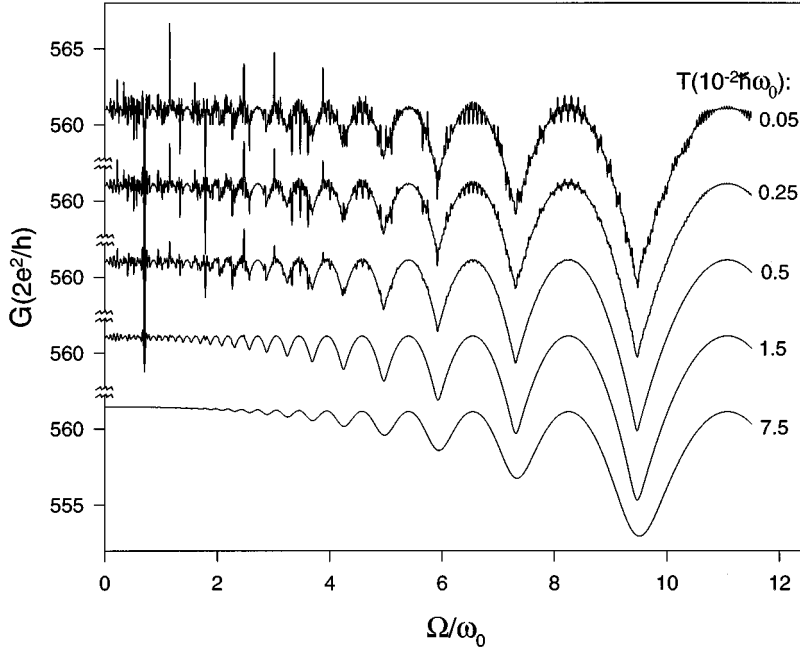
FIG. 7. Conductance (G, in units of $2e^2/h$) of a 3D symmetric contact vs cyclotron frequency (Ω, in units of ω_0), plotted for various values of the temperature (T, in units of $10^{-2}\hbar\omega_0$). Note that the AB oscillations vanish first in the strong-field region for $T \gtrsim \hbar\omega_0 \ (\omega_0/\Omega)$. AB oscillations in the weak-field region vanish at higher temperatures, $T \gtrsim \hbar\omega_0$. For all temperatures we used $\omega_0/\omega_z = 20$ and $\xi = 670$.

where $f_0(\epsilon)$ is the Fermi distribution function. An increase of the temperature leads to a smearing of the steps and to a decrease of the amplitude of the magnetic oscillations. It is of interest to note that the AB oscillations have different temperature dependencies in the case of weak $\Omega \ll \omega_0$,[12,13] and strong, $\omega_0 \ll \Omega$,[34] magnetic fields. The temperature dependence of the AB oscillations is determined by the function $\exp[-2\pi^2 T/T_0(H)]$, where for $T_0(H)$ we have[12,34]

$$T_0(H) \simeq \begin{cases} \hbar\omega_0, & \Omega \ll \omega_0 \\ \hbar\omega_0 \dfrac{\omega_0}{\Omega}, & \omega_0 \ll \Omega. \end{cases} \quad (20)$$

The magnetic-field dependence of the conductance at different temperatures, demonstrating, according to Eq. (20), damping (disappearance) of the AB oscillations first in the region of strong fields and subsequently, at higher temperatures, for weak ones, is plotted in Fig. 7.

2. Tilted and transverse magnetic fields

To investigate the case of tilted fields we chose for the magnetic-field orientation the yz plane, i.e., $\vec{H} = (0, H_y, H_z)$, with the following gauge of the vector potential:

$$\vec{A} = (zH_y - yH_z, 0, 0). \quad (21)$$

Transforming to a mixed momentum-coordinate representation ϕ, y, and z, where $\phi = p_x/\omega_x m^*$, Hamiltonian (15) may be written as

$$\mathcal{H}(\psi, y, z) = -\frac{\hbar^2}{2m^*} \left(\frac{\partial}{\partial\phi} \ \frac{\partial}{\partial y} \ \frac{\partial}{\partial z} \right) \underline{I} \begin{pmatrix} \partial/\partial\phi \\ \partial/\partial y \\ \partial/\partial z \end{pmatrix}$$

$$+ \frac{m^*}{2} (\phi y z) \underline{A} \begin{pmatrix} \phi \\ y \\ z \end{pmatrix}. \quad (22)$$

Here $\underline{I}$ is the unit matrix and the matrix $\underline{A}$ has the form

$$\underline{A} = \begin{pmatrix} \omega_x^2 & -\omega_x\Omega_z & \omega_x\Omega_y \\ -\omega_x\Omega_z & \omega_y^2 + \Omega_z^2 & -\Omega_y\Omega_z \\ \omega_x\Omega_y & -\Omega_y\Omega_z & -\omega_z^2 + \Omega_y^2 \end{pmatrix}, \quad (23)$$

with $\Omega_y = eH_y/m^*c$ and $\Omega_z = eH_z/m^*c$. Making a unitary transformation of the coordinates ϕ, y, and z, which diagonalizes the matrix $\underline{A}$, for the Hamiltonian in the new representation (q_1, q_2, q_3) we obtain the following expression:

$$\mathcal{H}(q_1, q_2, q_3) = \sum_{i=1}^{3} \left\{ -\frac{\hbar^2}{2m^*} \frac{\partial^2}{\partial q_i^2} + \frac{m^*}{2} \lambda_i q_i^2 \right\}. \quad (24)$$

Here λ_i are the eigenvalues of the matrix $\underline{A}$ (note that the matrix $\underline{A}$ is Hermitian, so that its eigenvalues are real) which may be determined from the equation

$$\lambda^3 + C_2\lambda^2 + C_1\lambda + C_0 = 0, \quad (25)$$

where

$$C_2 = -\omega_x^2 - \omega_y^2 + \omega_z^2 - \Omega_z^2 - \Omega_y^2,$$

$$C_1 = -\omega_z^2(\omega_x^2 + \omega_y^2 + \Omega_z^2) + \omega_y^2(\omega_x^2 + \Omega_y^2), \quad (26)$$
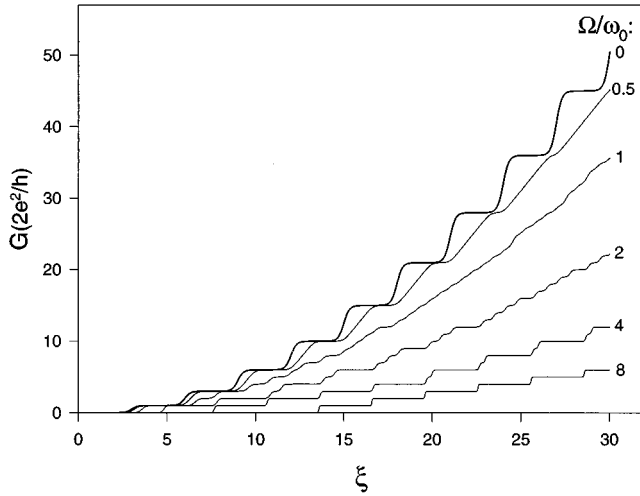
$$C_0 = \omega_x^2 \omega_y^2 \omega_z^2.$$

FIG. 8. Conductance (G, in units of $2e^2/h$) of a symmetric 3D point contact vs ξ in the presence of transverse magnetic fields of various strengths. Note the similarity of the behavior of the conductance at low fields to that shown for the constriction in longitudinal magnetic fields (see Fig. 4), and the improvement of the "quality" of the conductance quantization in the strong-field limit.

A simple analysis of Eqs. (25) and (26) shows that there exist two positive roots, $\lambda_1 = \omega_1^2$ and $\lambda_2 = \omega_2^2$, and one negative root, $\lambda_3 = -\omega_3^2$, of Eq. (25). This means that the Hamiltonian in Eq. (24) has the same form as the Hamiltonian in Eq. (2), but with different values of the effective frequencies ω_1, ω_2, and ω_3. It should be noted that for a tilted magnetic field the "longitudinal" frequency ω_3 depends on the field.

At first we consider the case of a transverse magnetic field, $H_y = H$, $H_z = 0$. For symmetric constrictions, $\omega_x = \omega_y = \omega_0$, the solutions of Eqs. (25) and (26) are given by the expressions

$$\omega_1^2 = \tfrac{1}{2}(\omega_0^2 - \omega_z^2 + \Omega^2)$$
$$+ \tfrac{1}{2}\sqrt{\Omega^4 + 2\Omega^2(\omega_0^2 - \omega_z^2) + (\omega_0^2 + \omega_z^2)^2},$$
$$\omega_2^2 = \omega_0^2, \qquad (27)$$
$$\omega_3^2 = \tfrac{1}{2}(-\omega_0^2 + \omega_z^2 - \Omega^2)$$
$$+ \tfrac{1}{2}\sqrt{\Omega^4 + 2\Omega^2(\omega_0^2 - \omega_z^2) + (\omega_0^2 + \omega_z^2)^2}.$$

Equations (26) and (27) allow us to calculate the conductance of the constriction in a transverse magnetic field. The dependence of the conductance on the energy, for different values of the magnetic field, is shown in Fig. 8. In the weak field region, $\Omega \ll \omega_0$, the influence of the transverse field is similar to that of the longitudinal one [compare Figs. 8 and 4(a)]. In this limit, from Eq. (27) we obtain

$$\omega_1 \simeq \omega_0\left(1 + \frac{1}{2}\frac{\Omega^2}{\omega_0^2 + \omega_z^2}\right), \qquad (28a)$$

$$\omega_3 \simeq \omega_z\left(1 - \frac{1}{2}\frac{\Omega^2}{\omega_0^2 + \omega_z^2}\right), \qquad (28b)$$

The magnetic field shifts one of the transverse frequencies, thus making the constriction effectively asymmetric. The lat-
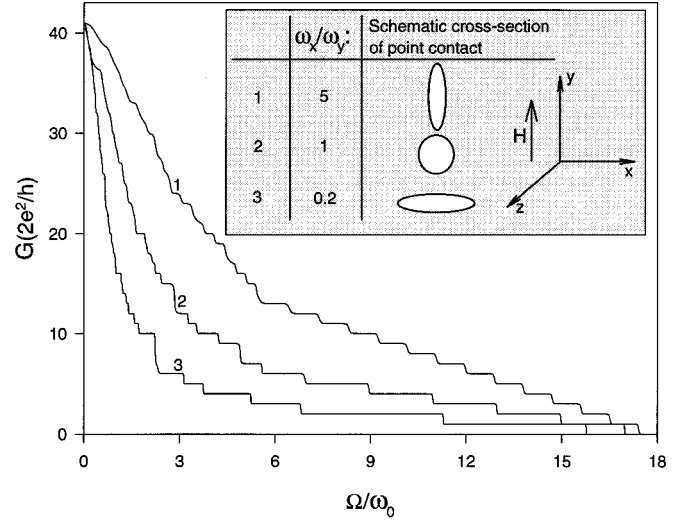

FIG. 9. Conductance (G, in units of $2e^2/h$) of 3D point contacts vs the strength of an applied transverse magnetic field (expressed in terms of Ω/ω_0), plotted for various values of ω_x/ω_y, while maintaining a constant value of the cross-sectional area of the constriction, i.e., $\omega_0 = \sqrt{\omega_x\omega_y}$. Here we used $\xi = 27$. The different behavior of the conductance, depending on the cross-sectional shape of the constriction, is due to different scenarios of depopulation of the magnetoelectric subbands.

ter may result in the removal of the degeneracy and even a smearing of the steps. The frequency ω_3 which determines the shape of the steps changes slightly.

In the strong-field region $\Omega \gg \omega_0$, from Eq. (27) we obtain

$$\omega_1 \simeq \Omega, \qquad \omega_3 \simeq \omega_z\frac{\omega_0}{\Omega}. \qquad (29)$$

The decrease of the frequency ω_3 with the strength of the magnetic field corresponds to an effective lengthening of the constriction. This implies that strong (transverse) magnetic fields enhance the quantization characteristics of the conductance. In a strong enough perpendicular magnetic field, conductance quantization can occur even in constrictions which do not exhibit such quantization under zero-field conditions. A similar effect of the influence of a strong magnetic field on the quantization of the conductance was discussed by Büttiker[25,26] for two-dimensional contacts.

As mentioned above, the steplike structure of the conductance is caused by changes in the number of transmitted channels. This can be achieved most easily by varying the magnitude of the magnetic field. In Fig. 9 we plotted the conductance of symmetric (curve 2) and asymmetric (curves 1 and 3) constrictions as a function of the strength of a transverse (oriented along the y direction) magnetic field, for a fixed value of the energy. Increase of the magnetic field leads to depopulation of the magnetoelectric subbands in the constriction, resulting in a steplike decrease of the conductance. Notice that the slopes of the steps become larger at higher values of the magnetic field.

The role of the confining potential describing the constriction in the process of the depopulation of the subbands may be readily demonstrated for asymmetric constrictions (note
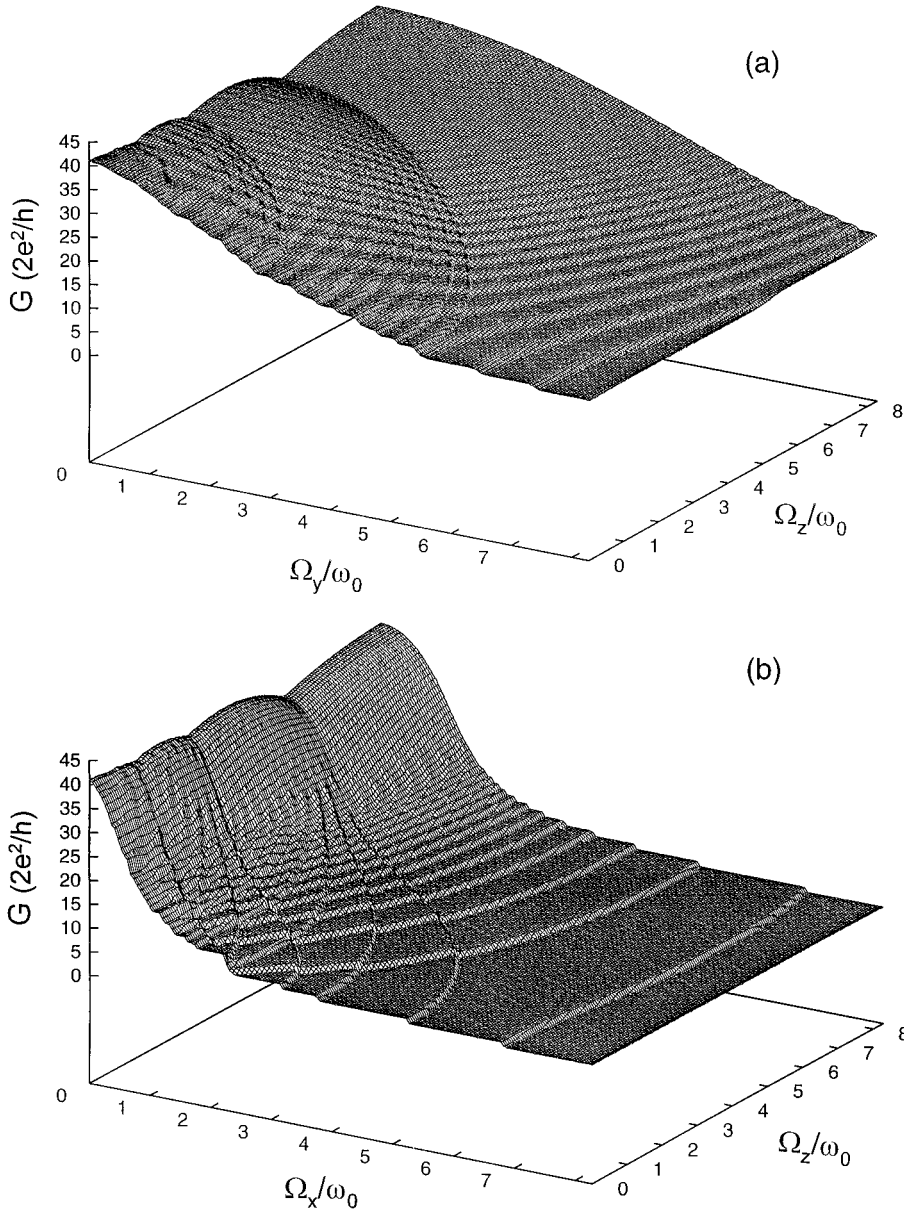
FIG. 10. Conductance (G, in units of $2e^2/h$) of a 3D constriction with the configuration denoted as 1 in Fig. 9, plotted as a function of a tilted magnetic field (in units of Ω/ω_0, with $\omega_0 = \sqrt{\omega_x \omega_y}$). Here we used $\xi = 27$ as in Fig. 9. (a) and (b) correspond to different orientations of the magnetic field; in (a) the applied field is in the yz plane, and in (b) in the xz plane. Note the coexistence of quantum oscillations (the AB and Shubnikov–de Haas effects) and the effect of the depopulation of the magnetoelectric subbands.

that the value of the cross-sectional area of the constriction is maintained constant, i.e., $\omega_x \omega_y = $ const., corresponding to a constant value of the classical conductance at zero field[1]). Different relative orientations of the transverse magnetic field with respect to the x and y axes lead to different field dependencies of the conductance (Fig. 9, curves 1 and 3). Such a behavior is due to different scenarios of the depopulation of the magnetoelectric subbands for different orientations of a transverse magnetic field relative to the cross-sectional axes of the contact. Depopulation of the subbands, leading to a decrease of the conductance, occurs earlier (i.e., for smaller field strength) for a magnetic field oriented along the small axis of the ellipsoidal cross section of the constriction. This effect is related to the decrease of the number of current-carrying edge modes with increasing strength of the applied magnetic field; for configuration 1 in Fig. 9 the number of propagating modes is larger than for configurations 2 and 3, and consequently the relative change in the conductance caused by the increase of the magnetic field is smaller for this configuration.

Finally, for an arbitrarily tilted orientation of the magnetic field the conductance of the constriction exhibits properties due to both the longitudinal (AB and Shubnikov–de Haas oscillations) and transverse (steplike decrease) components of the field. As a demonstration, in Fig. 10(a) we show the conductance of the constriction denoted as 1 in Fig. 9, for an applied magnetic field of arbitrary orientations in the yz plane. For longitudinal orientation of the magnetic field (i.e., vanishing value of $\Omega_y = eH_y/m^*c$), one observes AB oscillations for small values of $\Omega_z = eH_z/m^*c$, and Shubnikov–de Haas oscillations for larger ones [see Sec. II B 1]. For the transverse orientation of the field (i.e., $\Omega_z \simeq 0$) a steplike decrease of the conductance is seen (compare our discussion in connection with Fig. 9). In Fig. 10(b) the conductance for the same constriction, but for a magnetic field tilted in the xz plane (for this configuration the short axis of the elliptical cross section of the constriction lies in the plane of the magnetic field), is shown. The behavior of the conductance for longitudinal ($\Omega_x = 0$) orientation of the field is the same as in Fig. 10(a), while for a transverse

orientation the steplike decrease is faster than that in Fig. 10(a) (compare curves 1 and 3 in Fig. 9).

III. SUMMARY

The analysis which we performed demonstrated a variety of transport properties of 3D quantum constrictions. Certain properties of the electronic eigenvalue spectra, and consequently certain characteristics of conductance quantization, in such structures, depend on the nature of the confining potential describing the system. In particular, different potentials lead to different distributions of the eigenvalues as a function of the energy, and to different degrees of degeneracies of the spectrum. For example, in symmetric constrictions (i.e., contacts with circular cross sections) described by a hard-wall confining potential the spectrum is obtained as the zeros of the Bessel functions, and the conductance exhibits a stepwise structure with step heights of $2e^2/h$ or $2(2e^2/h)$, depending on the eigenvalue degeneracy.[17] On the other hand for similar constrictions described by a soft confining potential, such as the harmonic potential used in this paper, the conductance quantization steps are characterized by step heights proportional to the degree of degeneracy, which is equal in our model to the step number (see Fig. 2). In both cases the sharp step structure occurring in the absence of quantum tunneling, may be "smeared" when the tunneling effect on the transmission through the constriction is included, and the degree of such smearing of the conductance steps depends on the radius of curvature ("effective length") of the wire (see Figs. 1 and 2).

The presence of an additional parameter characterizing the shape of the cross section of the 3D constriction leads to a significant effect on the conductance quantization. In constrictions with an asymmetric transverse cross section the degeneracy may be removed. When a size of the plateau between successive steps becomes smaller than the smearing region of nondegenerate steps, the steplike structure of the conductance may disappear (Fig. 3). Such effects occur for both hard and soft confining potentials,[36] and may explain the occasional disappearance of steps in experiments on 3D quantum point contacts.[21]

Longitudinal magnetic fields change the character of ballistic electronic transport through the constriction leading to the appearance of AB oscillations in the conductance. In the strong magnetic fields, $\Omega \gg \omega_0$ ($r_c \ll d$, where d is the effective transverse size of the narrowing), the AB oscillations are superimposed on the Shubnikov–de Haas ones (Fig. 5).

Temperature damps the AB oscillations on a scale of $\hbar \omega_0 (\omega_0/\Omega)$ in strong fields and on a scale of $\hbar \omega_0$ in weak ones, $\Omega \ll \omega_0$ (Fig. 7). It is of interest to note that in such 3D systems there exists a correlation between conductance quantization and the AB effect. Both effects vanish in short constrictions (compare Figs. 2 and 6).

Transverse magnetic fields depopulate the magnetoelectric subbands created by the magnetic field and the confining potential, leading to a steplike decrease of the conductance of the constriction as a function of the field strength (Figs. 9 and 10).

The AB oscillations of the conductance of the quantum point contact may be observed in magnetic fields, such that the magnetic flux through the cross section of the contact is of the order of the flux quantum Φ_0, i.e.,

$$H \gtrsim \Phi_0/d^2. \tag{30}$$

For $H \sim 10^5$ G we obtain $d \gtrsim 10$ nm. The Shubnikov–de Haas oscillations appear in stronger magnetic fields or larger constrictions, such that the cyclotron radius of the electron is smaller than the effective transverse size (d) of the constriction, i.e.,

$$d \gtrsim \frac{m^* c v_F}{eH}. \tag{31}$$

For a magnetic field $H \sim 10^5$ G, we estimate $d \gtrsim 10^2$ nm.

[1] Yu. V. Sharvin, Zh. Éksp. Teor. Fiz. **48**, 984 (1965) [Sov. Phys. JETP **21**, 655 (1965)].

[2] I. K. Yanson, Zh. Éksp. Teor. Fiz. **66**, 1035 (1974) [Sov. Phys. JETP **39**, 506 (1974)].

[3] I. O. Kulik, A. N. Omelyanchuk, and R. I. Shekhter, Fiz. Nizk. Temp. **3**, 1543 (1977) [Sov. J. Low Temp. Phys. **3**, 789 (1977)].

[4] E. N. Bogachek, I. O. Kulik, and R. I. Shekhter, Solid State Commun. **56**, 999 (1985); E. N. Bogachek and R. I. Shekhter, Fiz. Nizk. Temp. **14**, 810 (1987) [Sov. J. Low Temp. Phys. **14**, 445 (1988)].

[5] H. M. Swartjes, A. P. van Gelder, A. G. M. Jansen, and P. Wyder, Phys. Rev. B **39**, 3086 (1989); I. K. Yanson, O. I. Shklyarevskii, and N. N. Gribov, J. Low Temp. Phys. **88**, 135 (1992); N. L. Bobrov, J. A. Kokkedee, N. N. Gribov, I. K. Yanson, and A. G. M. Jansen, Physica B **204**, 83 (1995).

[6] B. J. van Wees, H. van Houten, C. W. J. Beenakker, J. G. Williamson, L. P. Kouwenhoven, D. van der Marel, and C. T. Foxon, Phys. Rev. Lett. **60**, 848 (1988).

[7] D. A. Wharam, T. J. Thornton, R. Newbury, M. Pepper, H. Ahmed, J. E. F. Frost, D. G. Hasko, D. C. Peacock, D. A. Ritchie, and G. A. C. Jones, J. Phys. C **21**, L209 (1988).

[8] L. I. Glazman, G. B. Lesovik, D. E. Khmelnitskii, and R. I. Shekhter, Pis'ma Zh. Éksp. Teor. Fiz. **48**, 218 (1988) [JETP Lett. **48**, 238 (1988)].

[9] H. van Houten, C. W. J. Beenakker, and B. J. van Wees, Semicond. Semimet. **35**, 9 (1992).

[10] P. H. M. van Loosdrecht, C. W. J. Beenakker, H. van Houten, J. G. Williamson, B. J. van Wees, J. E. Mooij, C. T. Foxon, and J. J. Harris, Phys. Rev. B **38**, 10 162 (1988).

[11] L. I. Glazman and M. Jonson, Phys. Rev. B **41**, 10 686 (1990).

[12] E. N. Bogachek and G. A. Gogadze, Zh. Éksp. Teor. Fiz. **63**, 1839 (1972) [Sov. Phys. JETP **36**, 973 (1973)].

[13] E. N. Bogachek, Fiz. Nizk. Temp. **2**, 473 (1976) [Sov. J. Low Temp. Phys. **2**, 235 (1976)].

[14] N. B. Brandt, D. V. Gitsu, A. A. Nikolayeva, and Ya. G. Ponomarev, Pis'ma Zh. Éksp. Teor. Fiz. **24**, 304 (1976) [JETP Lett. **24**, 272 (1976)]; Zh. Éksp. Teor. Fiz. **72**, 2332 (1977) [Sov. Phys. JETP **45**, 1226 (1977)]; N. B. Brandt, E. N. Bogachek, D. V. Gitsu, G. A. Gogadze, I. O. Kulik, A. A. Nikolayeva, and Ya. G. Ponomarev, Fiz. Nizk. Temp. **8**, 718 (1982) [Sov. J. Low Temp. Phys. **8**, 358 (1982)].

[15] U. Landman, W. D. Luedtke, N. A. Burnham, and R. J. Colton, Science **248**, 454 (1990).

[16] U. Landman and W. D. Luedtke, J. Vac. Sci. Technol. B **9**, 414 (1991).

[17] E. N. Bogachek, A. M. Zagoskin, and I. O. Kulik, Fiz. Nizk. Temp. **16**, 1404 (1990) [Sov. J. Low Temp. Phys. **16**, 796 (1990)].

[18] J. A. Torres, J. I. Pascual, and J. J. Saenz, Phys. Rev. B **49**, 16 581 (1994), where some of the results of Ref. 17 have been reproduced.

[19] E. N. Bogachek, M. Jonson, R. I. Shekhter, and T. Swahn, Phys. Rev. B **47**, 16 635 (1993); **50**, 18 341 (1994).

[20] J. I. Pascual, J. Mendez, J. Gomez-Herrero, A. M. Baro, N. Garcia, and Vu Thien Binh, Phys. Rev. Lett. **71**, 1852 (1993).

[21] J. I. Pascual, J. Mendez, J. Gomez-Herrero, A. M. Baro, N. Garcia, U. Landman, W. D. Luedtke, E. N. Bogachek, and H.-P. Cheng, Science **267**, 1793 (1995); J. Vac. Sci. Technol. B **13**, 1280 (1995).

[22] L. Olesen, E. Laegsgaard, I. Stensgaard, F. Besenbacher, J. Schiotz, P. Stoltze, K. W. Jacobsen, and J. N. Norskov, Phys. Rev. Lett. **72**, 2251 (1994).

[23] N. Agrait, J. G. Rodrigo, and S. Vieira, Phys. Rev. B **47**, 12 345 (1993).

[24] J. M. Krans, C. J. Muller, I. K. Yanson, Th. C. M. Govaert, R. Hesper, and J. M. van Ruitenbeek, Phys. Rev. B **48**, 14 721 (1993); C. J. Muller, J. M. van Ruitenbeek, C. W. J. Beenakker, and R. de Bruyn Ouboter, Physica B **189**, 225 (1993); J. M. Krans, J. M. van Ruitenbeek, V. V. Fisun, I. K. Yanson, and L. J. de Jongh, Nature **375**, 767 (1995).

[25] M. Büttiker, Phys. Rev. B **41**, 7906 (1990).

[26] M. Büttiker, Semicond. Semimet. **35**, 19 (1992).

[27] Transmission probability for the harmonic-type potential was calculated by Kemble [see, for example, L. D. Landau and E. M. Lifshitz, *Quantum Mechanics* (Pergamon, Oxford, 1977)].

[28] R. Landauer, Philos. Mag. **21**, 863 (1970).

[29] Y. Imry, in *Directions in Condensed Matter Physics*, edited by G. Grinstein and G. Mazenko (World Scientific, Singapore, 1986), p. 101.

[30] B. Schuh, J. Phys. A **18**, 803 (1985).

[31] V. Fock, Z. Phys. **47**, 446 (1928); C. G. Darwin, Proc. Cambridge Philos. Soc. **27**, 86 (1930).

[32] U. Sivan and Y. Imry, Phys. Rev. Lett. **61**, 1991 (1988).

[33] Y. Meir, O. Entin-Wohlman, and Y. Gefen, Phys. Rev. B **42**, 8351 (1990).

[34] E. N. Bogachek and U. Landman, Phys. Rev. B **52**, 14 067 (1995).

[35] G. Kirczenow, A. S. Sachrajda, Y. Feng, R. P. Taylor, L. Henning, J. Wang, P. Zawadzki, and P. T. Coleridge, Phys. Rev. Lett. **72**, 2069 (1994); G. Kirczenow, Phys. Rev. B **50**, 1649 (1994).

[36] For a comparative study of shape effects on conductance quantization in three-dimensional constrictions described by soft and hard confining potentials (with and without applied magnetic field), showing a dependence of such effects on the spectral energy distribution of the eigenvalues and their degeneracies, see A. G. Scherbakov, E. N. Bogachek, and U. Landman (unpublished).